JOURNAL OF PROPULSION AND POWER
Vol. 17, No. 2, March–April 2001

Control of Blade Flutter by Smart-Casing Treatment

Xiaofeng Sun,* Xiaodong Jing,† and Hongwu Zhao‡
Beijing University of Aeronautics and Astronautics, Beijing 100083, People's Republic of China

A novel acoustic liner with adjustable impedance is introduced as a casing treatment to suppress compressor blade flutter. Numerical results are presented to show the variation of the fluctuating lift and moment coefficients as functions of the liner cavity depth and the bias-flow Mach number through the orifices of the liner. It can be seen from these results that liners with different impedances would have an either positive or negative effect on compressor blade flutter under a given compressor working condition. However, an optimal impedance value that matches a specific working condition to suppress the blade flutter can be found by a numerical method. Correspondingly, two curves that determine the control values of liner cavity depth and bias-flow Mach numbers under any given compressor working condition can be obtained. By means of these control curves, it is proposed that the active control of compressor blade flutter may be realized by a feedforward control methodology. Compared with the existing methods for the control of blade flutter, smart-casing treatment indeed shows a novel conception of blade flutter control.

Nomenclature

A_{ab}	=	periphery of a blade
A_b	=	the upper or lower surface of a blade
a_0	=	speed of sound
b	=	blade semichord
C_{Fqi}, $C_{F\alpha i}$	=	imaginary part of blade lift coefficient
C_{Fqr}, $C_{F\alpha r}$	=	real part of blade lift coefficient
C_{Mqi}, $C_{M\alpha i}$	=	imaginary part of blade moment coeficient
C_{Mqr}, $C_{M\alpha r}$	=	real part of blade moment coefficient
G	=	the Green's function
G_ω	=	Fourier transform of the Green's function for time
h	=	height from the hub to the tip in the transformed space
k_b	=	wave number, $k_b = \omega_b/a_0$
L	=	liner cavity depth
M_{bias}	=	the Mach number of the bias flow
M_r	=	mean-flow Mach number in chordwise direction
M_t	=	blade circumferential Mach number in mean radius
M_x	=	Mach number in x' direction
M_y	=	Mach number in negative y' direction
$\bar{p}_m$	=	amplitude of perturbation pressure for mth blade
r	=	(x, y, z)
r_0	=	(x_0, y_0, z_0)
r_m	=	mean radius of blades
t	=	time in an observer point
U_r	=	mean velocity in chordwise direction
u	=	velocity perturbation in x direction
v	=	velocity perturbation in y direction
w	=	velocity perturbation in z direction
x, y, z	=	a blade-fixed coordinate system for an observer
x_0, y_0, z_0	=	a blade-fixed coordinate system for a source
x', y', z'	=	a duct-fixed coordinate system
z_a	=	acoustic impedance of perforated liner with bias flow
α	=	wave number in ξ direction
α'	=	wave number in x' direction
β	=	wave number in η direction
β_a	=	wall admittance
β'	=	wave number in y' direction
θ	=	blade-stagger angle
λ	=	reduced frequency based on blade chord
ξ, η, ζ	=	a blade-fixed coordinate system for an observer in the transformed space
ξ_0, η_0, ζ_0	=	a blade-fixed coordinate system for a source in the transformed space
ρ	=	perturbation density
σ	=	interblade phase angle
Ω	=	rotating speed of rotor
ω	=	angular frequency
ω_b	=	perturbation frequency of blade force

Received 20 April 1999; revision received 7 January 2000; accepted for publication 12 June 2000.

*Professor, Department of Jet Propulsion, Box 407; sunxf@ns.ngl.buaa.edu.cn. Member AIAA.

†Ph.D. Candidate, Department of Jet Propulsion, Box 407; jxd@ns.ngl.buaa.edu.cn.

‡Ph.D. Candidate, Department of Jet Propulsion, Box 407; zhw@ns.ngl.buaa.edu.cn.

Introduction

DESPITE considerable research effort in the area of turbomachinery aeroelasticity over the past few decades, flutter is still occurring in current technology engines and research fans. Once encountered, these instabilities have often proved very troublesome to eliminate, requiring costly and time-consuming testing and redesign efforts. A lot of work had been done to find ways for suppressing compressor blade flutter. Most of these proposed methods fall into three main categories[1]: 1) mistuning, 2) aeroelastic tailoring, and 3) dry friction damping or mode-shape control. In addition, a novel way of controlling blade flutter by use of a nonrigid wall or a soft wall was suggested by Watanabe and Kaji[2] and Namba et al.,[3] respectively, in 1984. Their research objective was to try to find a kind of flutter-suppressing liner. In fact, if this is verified as feasible, there is at least one advantage to using an acoustic liner to suppress compressor flutter, i.e., the application of flutter-suppressing liners may not cause any apparent aerodynamic loss or weight penalty as a passive flutter-control way compared with the existing methods. More recently, Sun and Kaji[4] made a further numerical investigation of the influence of a soft wall on blade flutter instability in a supersonic cascade with a subsonic leading-edge locus by solving an upwash integral equation with a directly coupling boundary condition. Their results all show that a nonrigid wall has indeed less or more influence on the unsteady pressure distribution and aeroelastic stability of blades, depending on the aerodynamic and geometrical parameters of cascade and the range of the acoustic admittance value of the wall. It is known that all the methods mentioned above are based on the conception of passive control. According to the existing experimental or numerical results, some of these methods work very well to suppress compressor flutter under the given condition.

However, once the compressor works off this given condition, the effectiveness of passive control in suppressing compressor blade flutter will drop greatly; some passive flutter-suppressing methods even have negative effects. In addition, it is worth noting that most of the passive flutter-suppressing methods are achieved at the cost of compressor efficiency. So, as a new conception of suppressing compressor flutter, active flutter control has been of great concern in recent years. In fact, there have been many investigations about the active control of isolated airfoil flutter, which is carried out by means of the feedback-control method with loudspeakers or piezoelectrical materials installed on the airfoil surface or wall as actuators, as in the work presented by Huang.[5] Therefore how to find a new method for the active control of rotating blade flutter in compressors has become a problem of interest. A possible way suggested by the present investigation is to extend the passive flutter control through a flutter-suppressing liner to an active way. However, it is noted that all these studies[2–4] are based on a fixed-wall-impedance condition and there is no connection with a specific impedance model. To realize the active control of compressor flutter by this method, an adjustable-wall-impedance model must be given. In addition, how to realize this active control must also be resolved.

It has been found that there is a kind of liner with adjustable impedance, which consists of a perforated plate with bias flow through the orifices. Recent experimental and theoretical work has shown that such a liner would be a good prospect for many applications. Therefore there is reason to believe that, supposing a kind of flutter-suppressing liner with adjustable impedance is available, it would be possible to realize the active control of compressor blade flutter. In fact, the progress made on vortex sound interaction has revealed some possibility of designing such an acoustic liner. The theoretical and experimental investigations developed at the end of the 1970s[6,7] have shown that the interaction between a sound wave and a low Mach number mean flow at a trailing edge can result in sound absorption, and the acoustical energy is converted into unsteady vortical motion, which is convected away by the mean flow. In 1990 Hughes and Dowling[8] further showed the sound-absorption coefficient or impedance of a liner can be effectively controlled by adjusting the speed of bias flow and the experimental results are in very good agreement with the theoretical calculation. In addition, Jing and Sun[9] made some further parametric studies on the factors that influence the sound-absorption coefficient, which also showed a good agreement with experimental results. More recently, Zhao and Sun[10] designed an active control system of wall impedance for this kind of liner by means of a standing-wave tube and showed how to obtain an optimal sound-absorption coefficient or a specific impedance condition under the idealized condition.

On the basis of what has been found, the objective of the present investigation is to couple the existing unsteady aerodynamics model with an acoustic model to show further the possibility of controlling the compressor blade flutter by changing control variables such as the velocity of bias flow and the geometry of the liner. This may be taken as a first step toward designing a real active-control system. Hence our main concern in this paper is to give a real wall-impedance model and discuss the control strategy for a smart-casing treatment based on a more extensive numerical investigation.

Formulations

Basic Equations

Consider a three-dimensional cascade with blades that are assumed to be flat plates of negligible thickness (Fig. 1). The blades in the cascade are assumed to perform identical harmonic motions of small amplitude with a constant phase angle between the motion of adjacent blades. The mean positions of the blade are aligned parallel to the freestream flow. The flow is subsonic and assumed to be isentropic and frictionless.

The perturbation pressure p induced by the motion of the blades is then governed by the wave equation

$$\left(1-M_r^2\right)\frac{\partial^2 p}{\partial x^2}+\frac{\partial^2 p}{\partial y^2}+\frac{\partial^2 p}{\partial z^2}-\frac{1}{a_0^2}\frac{\partial^2 p}{\partial t^2}-\frac{2M_r}{a_0}\frac{\partial^2 p}{\partial x\,\partial t}=0 \quad (1)$$

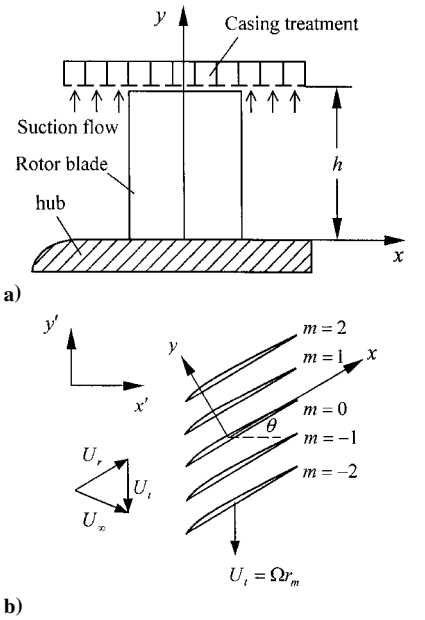

Fig. 1 Cascade model.

Green's Function in a Lined Duct

The Green's function of Eq. (1) is

$$\left(1-M_r^2\right)\frac{\partial^2 G}{\partial x_0^2}+\frac{\partial^2 G}{\partial y_0^2}+\frac{\partial^2 G}{\partial z_0^2}-\frac{1}{a_0^2}\frac{\partial^2 G}{\partial \tau^2}-\frac{2M_r}{a_0}\frac{\partial^2 G}{\partial x_0\,\partial \tau}$$
$$=-\delta(t-\tau)\delta(\boldsymbol{r}-\boldsymbol{r}_0) \quad (2)$$

According to the generalized Green's function theory,[11] the solution of Eq. (1) can be expressed as

$$p(\boldsymbol{x},t)=\int_{-T}^{T}\mathrm{d}\tau\int_A\left[G\left(\frac{\partial}{\partial n}+\frac{V_n}{a_0^2}\frac{\mathrm{D}_0}{\mathrm{D}\tau}\right)p(\boldsymbol{y},\tau)\right.$$
$$\left.-p(\boldsymbol{y},\tau)\left(\frac{\partial}{\partial n}+\frac{V_n}{a_0^2}\frac{\mathrm{D}_0}{\mathrm{D}\tau}\right)G(\boldsymbol{y},\tau\,|\,\boldsymbol{x},t)\right]\mathrm{d}S(\boldsymbol{y}) \quad (3)$$

Suppose that G_ω represents the Fourier transforms of the Green's function in Eq. (2). Introducing the following coordinate transforms, $\xi=x/b$, $\eta=y\beta_r/b$, and $\zeta=z\beta_r/b$, and then substituting $G_\omega=G'_\omega e^{iKM_r\xi}$ into Eq. (2) yields

$$\frac{\partial^2 G'_\omega}{\partial \xi_0^2}+\frac{\partial^2 G'_\omega}{\partial \eta_0^2}+\frac{\partial^2 G'_\omega}{\partial \zeta_0^2}+K^2G'_\omega=-\frac{b^2}{\beta_r^2}e^{-i(\omega t+KM_r\xi_0)}\delta(\boldsymbol{r}-\boldsymbol{r}_0) \quad (4)$$

where $K=\omega b/a_0\beta_r^2$ and $\beta_r=\sqrt{(1-M_r^2)}$. Using double Fourier transforms defined by

$$G'_\omega(\alpha,\beta,\zeta_0/\xi,\eta,\zeta)$$
$$=\int_{-\infty}^{+\infty}\int_{-\infty}^{+\infty}G'_\omega\left(\frac{\boldsymbol{r}_0}{\boldsymbol{r}}\right)e^{-i(\alpha\xi_0+\beta\eta_0)}\,\mathrm{d}\xi_0\,\mathrm{d}\eta_0 \quad (5)$$

gives

$$\left(\frac{\partial^2}{\partial \zeta_0^2}+K_q^2\right)G'_\omega\left(\alpha,\beta,\frac{\zeta_0}{\xi},\eta,\zeta\right)$$
$$=-\frac{1}{\beta_r}e^{-i[\omega t+(\alpha+KM_r)\xi+\beta\eta]}\delta\left[\frac{b}{\beta_r}(\zeta-\zeta_0)\right] \quad (6)$$

where $K_q^2=K^2-\alpha^2-\beta^2$. The solution of Eq. (6) is

$$G'_\omega=A\cos K_q\zeta_0+B\sin K_q\zeta_0-\frac{e^{-i[\omega t+(\alpha+KM_r)\xi+\beta\eta]}}{bK_q}$$
$$\times\begin{cases}\cos K_q\zeta_0\sin K_q\zeta, & \zeta_0\le\zeta\\ \cos K_q\zeta\sin K_q\zeta_0, & \zeta_0\ge\zeta\end{cases} \quad (7)$$

To determine the constants A and B, the boundary condition on the liner surface is needed. The liner can be modeled by a vortex sheet separating the uniform mean-flow region within the duct from the no-flow region in the liner.[12] The two regions are coupled by matching the pressure and the particle displacement. A duct-fixed coordinate system is introduced, which is related to the rotating coordinates as follows:

$$x = x' \cos\theta + (y' + \Omega r_m \tau)\sin\theta$$
$$y = -x' \sin\theta + (y' + \Omega r_m \tau)\cos\theta, \qquad z = z' \tag{8}$$

With the continuity of the pressure and the particle displacement, the following boundary condition on the inner surface of the duct can be derived:

$$\frac{\partial p}{\partial z'} + i\beta_a k_0' \left(1 + \frac{\alpha'}{k_0'} M_x - \frac{\beta'}{k_0'} M_y\right)^2 p = 0 \tag{9}$$

Let

$$\Delta_{\zeta_0}(G_\omega) = \frac{\beta_r}{b}\frac{\partial G_\omega}{\partial \zeta_0} + i\beta_a k_0' \left(1 + \frac{\alpha'}{k_0'} M_x - \frac{\beta'}{k_0'} M_y\right)^2 G_\omega \bigg|_{\zeta_0 = h} = 0 \tag{10}$$

where $k_0' = \omega'/a_0$, $\omega' = \omega + (\beta' r_m)\Omega$. Besides, assume the hub is impermeable, so that

$$\frac{\partial G_\omega}{\partial \zeta_0}\bigg|_{\zeta_0 = 0} = 0 \tag{11}$$

With the condition given by Eqs. (10) and (11), it is easy to show that the constants are

$$A = \frac{\Delta_h(\sin K_q \zeta_0)\cos K_q \zeta_0 e^{-i[\omega t + (\alpha + KM_r)\xi + \beta\eta]}}{bK_q \Delta_h(\cos K_q \zeta_0)}, \qquad B = 0 \tag{12}$$

Therefore the Green's function can be written as

$$G = \frac{1}{(2\pi)^3}\int_{-\infty}^{+\infty}\int_{-\infty}^{+\infty}\int_{-\infty}^{+\infty}\left[\frac{\cos K_q\zeta \cos K_q\zeta_0 \Delta_h(\sin K_q\zeta_0)}{bK_q\Delta_h(\cos K_q\zeta_0)} - \frac{1}{bK_q}\begin{Bmatrix}\cos K_q\zeta_0 \sin K_q\zeta, & \zeta_0 \le \zeta \\ \cos K_q\zeta \sin K_q\zeta_0, & \zeta_0 \ge \zeta\end{Bmatrix}\right] \times e^{i\omega(\tau - t) + i(\alpha + KM_x)(\xi_0 - \xi) + i\beta(\eta_0 - \eta)}\, d\alpha\, d\beta\, d\omega \tag{13}$$

Pressure-Wave Solutions

By use of the impermeability condition on the blade and the wall boundary condition of duct, Eq. (3) then reduces to

$$p(\boldsymbol{x}, t) = \int_{-T}^{T} d\tau \int_{A_{db}} \left(-p\frac{\partial G}{\partial n}\right) ds(\boldsymbol{y}) \tag{14}$$

Let

$$\Delta p(\xi_0, \zeta_0, \tau) = p^-(\xi_0, \zeta_0, \tau) - p^+(\xi_0, \zeta_0, \tau) \tag{15}$$

where Δp is the pressure difference between the lower and the upper surfaces of a blade. Assume that the blade force changes with time dependence $\exp(i\omega_b \tau)$, i.e.,

$$\Delta p(\xi_0, \zeta_0, \tau) = \Delta\bar{p}(\xi_0, \zeta_0) e^{i\omega_b \tau} \tag{16}$$

hence

$$p(\boldsymbol{x}, t) = -\int_{-T}^{T} d\tau \int_{A_b} \Delta p(\xi_0, \zeta_0, \tau)\left(\frac{\beta_r}{b}\right)\frac{\partial G}{\partial \eta_0}\, dS \tag{17}$$

Carrying out the integration of τ leads to

$$p(\boldsymbol{x}, t) = \frac{-1}{(2\pi)^2}\int_{A_b}\int_{-\infty}^{+\infty}\int_{-\infty}^{+\infty} \Delta\bar{p}(\xi_0, \zeta_0) \times \left[\frac{\cos K_q\zeta \cos K_q\zeta_0 \Delta_h(\sin K_q\zeta_0)}{bK_q\Delta_h(\cos K_q\zeta_0)} - \frac{1}{bK_q}\begin{Bmatrix}\cos K_q\zeta_0 \sin K_q\zeta, & \zeta_0 \le \zeta \\ \cos K_q\zeta \sin K_q\zeta_0, & \zeta_0 \ge \zeta\end{Bmatrix}\right]\left(i\beta\frac{\beta_r}{b}\right) \times e^{i\omega_b t + i(\alpha - K_b M_r)(\xi_0 - \xi) + i\beta(\eta_0 - \eta)}\, d\alpha\, d\beta\, dS \tag{18}$$

The theory of residues can be used to evaluate the integration of β; hence,

$$p(\boldsymbol{x}, t) = -\mathrm{sgn}(\eta - \eta_0)\frac{\beta_r}{4\pi b^2 h}\int_{A_b}\int_{-\infty}^{+\infty} \Delta\bar{p}(\xi_0, \zeta_0) \times \sum_{q=1}^{+\infty}\left(\frac{\cos K_q\zeta \cos K_q\zeta_0}{\Lambda^\pm} \times e^{i\omega_b t - i(\alpha - K_b M_r)(\xi - \xi_0) - i\sqrt{K_b^2 - \alpha^2 - K_q^2}\,|\eta - \eta_0|}\right) d\alpha\, dS \tag{19}$$

For the mth blade, as shown in Fig. 1,

$$\bar{p}_m = -\mathrm{sgn}(\eta_m)\frac{\beta_r}{4\pi b^2 h}\int_{A_b}\int_{-\infty}^{+\infty} \times \sum_{q=1}^{+\infty}\left[\frac{\cos K_q\zeta \cos K_q\zeta_0}{\Lambda^\pm}\Delta\bar{p}_m(\xi_{0m}, \zeta_{0m}) \times e^{-i(\alpha - K_b M_r)[\xi - (\xi_0 + mh_1)] - i\sqrt{K_b^2 - \alpha^2 - K_q^2}\,|\eta - mh_2\beta_r|}\right] d\alpha\, dS \tag{20}$$

Assume that

$$\Delta\bar{p}_m(\xi_{0m}, \zeta_{0m}) = \Delta\bar{p}_0(\xi_0, \zeta_0) e^{im\sigma} \tag{21}$$

The complete solution to Eq. (1) is expressed simply as a sum of function $\bar{p}_m$ or all the blades, i.e.,

$$\bar{p} = -\frac{\beta_r}{4\pi b^2 h}\int_{A_b}\int_{-\infty}^{+\infty} \Delta\bar{p}_0(\xi_0, \zeta_0) \times \sum_{q=1}^{+\infty}\left[\frac{\cos K_q\zeta \cos K_q\zeta_0}{\Lambda^\pm}\sum_{m=-\infty}^{m=+\infty}\mathrm{sgn}(\eta_m) \times e^{im\sigma - i(\alpha - K_b M_r)[\xi - (\xi_0 + mh_1)] - i\sqrt{K_b^2 - \alpha^2 - K_q^2}|\eta - mh_2\beta_r|}\right] d\alpha\, dS \tag{22}$$

Upwash Integral Equation

The perturbation velocity v can be obtained from the linearized momentum equation in the form

$$\frac{\bar{v}(\xi, \eta, \zeta)}{U_r} = \int_0^1\int_{-1}^{1} f(\xi_0, \zeta_0) K(\xi - \xi_0, \eta, \zeta\,|\,\zeta_0)\, d\xi_0\, d\zeta_0 \tag{23}$$

Table 1 Lift and moment coefficients[a]

	Bending		Torsion	
λ	C_{Fq}	C_{Mq}	$C_{F\alpha}$	$C_{M\alpha}$
1.0	$-0.7191+i0.0672$	$0.1509-i0.1405$	$-0.8236-i0.0840$	$0.1824-i0.1483$
	$-0.7190+i0.0670$	$0.1511-i0.1405$	$-0.8235-i0.0838$	$0.1825-i0.1482$
1.2	$-0.7502+i0.0960$	$0.1328-i0.1288$	$-0.9048-i0.0634$	$0.1734-i0.1934$
	$-0.7500+i0.0957$	$0.1329-i0.1287$	$-0.9044-i0.0636$	$0.1735-i0.1932$
1.4	$-0.3470+i0.4620$	$-0.0269-i0.1198$	$-0.5147-i0.4997$	$-0.0257-i0.2328$
	$-0.3473+i0.4618$	$-0.0269-i0.1199$	$-0.5149-i0.4992$	$-0.0253-i0.2327$

[a]The first row gives the results from Ref. 13 for a given reduced frequency λ; the second row gives the results of the present program. $\sigma = 3.14$, $\theta = 0$, space/chord = 3.8, $M_r = 0.5$.

where

$$f(\xi_0, \zeta_0) = \frac{\Delta \bar{p}_0(\xi_0, \zeta_0)}{\rho_0 U_r^2}$$

$$K(\xi - \xi_0, \eta, \zeta \mid \zeta_0) = \frac{i\beta_r}{4\pi}\frac{\partial}{\partial \eta}\int_{-\infty}^{+\infty}\sum_{q=1}^{+\infty}\left[\frac{\cos K_q\zeta \cos K_q\zeta_0}{\Lambda^{\pm}(\alpha - K_b/M_r)}\sum_{m=-\infty}^{m=\infty}\operatorname{sgn}(\eta_m) \times e^{im\sigma - i(\alpha - K_bM_r)[\xi - (\xi_0 + mh_1)] - i\sqrt{K_b^2 - \alpha^2 - K_q^2}|\eta - mh_2\beta_r|}\right]d\alpha$$

$$\Lambda^{\pm} = \frac{1}{2}\left(1 + \frac{\sin 2K_qh}{2K_qh}\right) + \Lambda_1(\alpha, \beta^{\pm}) + \Lambda_2(\alpha, \beta^{\pm})$$

$$\beta^- = -\sqrt{K_b^2 - \alpha^2 - K_q^2}, \qquad \beta^+ = \sqrt{K_b^2 - \alpha^2 - K_q^2}$$

$$\Lambda_1(\alpha, \beta) = -\frac{i\beta_aM_r}{\alpha h\beta_r}\left(1 + \frac{\alpha'}{k_0'}M_x - \frac{\beta'}{k_0'}M_y\right)\cos^2 K_qh$$

$$\Lambda_2(\alpha, \beta) = \frac{i\beta_aM_t}{2h\beta_r}\left(1 + \frac{\alpha'}{k_0'}M_x - \frac{\beta'}{k_0'}M_y\right)^2 \times \left(\frac{\sin\theta}{\alpha} - \frac{\beta_r\cos\theta}{\beta}\right)\cos^2 K_qh$$

By letting $\eta \to 0$, we can express an integral equation for the pressure across the 0th blade in terms of the known upwash velocity on the blade surface as

$$\frac{\bar{v}(\xi, 0, \zeta)}{U_r} = \int_0^1\int_{-1}^1 f(\xi_0, \zeta_0)K_0(\xi - \xi_0, \zeta \mid \zeta_0)\,d\xi_0\,d\zeta_0 \tag{24}$$

where

$$K_0(\xi - \xi_0, \zeta \mid \zeta_0) = \lim_{\eta \to 0} K(\xi - \xi_0, \eta, \zeta \mid \zeta_0)$$

It can be further shown that

$$K(\xi - \xi_0, \zeta \mid \zeta_0) = \frac{i\beta_r}{4\pi}\lim_{\eta \to 0}\frac{\partial}{\partial \eta} \times \int_{-\infty}^{+\infty}\sum_{q=1}^{+\infty}\frac{\cos K_q\zeta \cos K_q\zeta_0 e^{-i(\alpha - K_bM_r)(\xi - \xi_0)}}{\alpha - K_b/M_r} \times \frac{1}{2i}\left(\frac{e^{i\sqrt{K^2 - \alpha^2 - K_q^2}\eta}e^{(i/2)\Delta_-}}{\Lambda^-\sin\frac{1}{2}\Delta_-} + \frac{e^{-i\sqrt{K^2 - \alpha^2 - K_q^2}\eta}e^{(i/2)\Delta_+}}{\Lambda^+\sin\frac{1}{2}\Delta_+}\right)d\alpha \tag{25}$$

where

$$\Delta_- = (\Gamma + h_1\alpha) + h_2\beta_r\beta^-$$

$$\Delta_+ = (\Gamma + h_1\alpha) + h_2\beta_r\beta^+, \qquad \Gamma = \sigma - K_bM_rh_1$$

For the kernel function defined in Eq. (25), some further mathematical treatments are needed for the numerical calculation, and then the method of collocation is used to solve the upwash integral equation.[3,4] Therefore the pressure difference distribution between the upper and the lower blade surfaces can be obtained, which is necessary for calculating the lift and the moment coefficients of blades.

Blade Lift and Moment Coefficients

For a bending vibration, the blade lift and moment coefficients are defined by

$$C_{Fq} = \frac{1}{\rho_0U_r\bar{v}_bHb}\int_0^1\int_0^\pi \Delta\bar{p}(\xi_0, \zeta_0)\,d\xi_0\,d\zeta_0 \tag{26}$$

$$C_{Mq} = \frac{1}{\rho_0U_r\bar{v}_bHb^2}\int_0^1\int_0^\pi \xi_0\Delta\bar{p}(\xi_0, \zeta_0)\,d\xi_0\,d\zeta_0 \tag{27}$$

and also for a torsional vibration, the definitions of the blade lift and moment coefficients are

$$C_{F\alpha} = \frac{1}{\rho_0U_r^2\alpha_tHb}\int_0^1\int_0^\pi \Delta\bar{p}(\xi_0, \zeta_0)\,d\xi_0\,d\zeta_0 \tag{28}$$

$$C_{M\alpha} = \frac{1}{\rho_0U_r^2\alpha_tHb^2}\int_0^1\int_0^\pi \xi_0\Delta\bar{p}(\xi_0, \zeta_0)\,d\xi_0\,d\zeta_0 \tag{29}$$

where $\bar{v}_b$ represents the amplitude of upwash velocity that is due to bending vibration and α_t is the amplitude of the angular displacement that is due to the torsional vibration of a blade.

It is well known that the imaginary part of the moment coefficient $C_{M\alpha i}$ will determine whether the blade flutters or not, i.e., if $C_{M\alpha l} < 0$, the system is stable; otherwise it is unstable. On the other hand, it is noted the radial standing waves will have no contribution to the integration of blade pressure distribution under a hard-wall condition. Therefore it can be concluded that the results of solving the three-dimensional integral equation for a hard wall will be the same as that from two-dimensional models in terms of the preceding definition of the lift and the moment coefficients. For the confirmation of reliabilities of the present model, Table 1 gives the results of solving the present three-dimensional integral equation and that from Ref. 13, which show very good agreement between each other.

Acoustic Impedance Model of Liner

In this study an acoustic liner with adjustable impedance is used to provide the soft-wall boundary condition. The acoustic liner is made of a perforated liner with bias flow (blow or suction) through it. The acoustic properties of this kind of acoustic liner have been investigated in detail in Refs. 6–9. Furthermore, Zhao and Sun[10] showed that the impedance of this kind of acoustic liner can be adjusted to a prescribed value through controlling the bias-flow velocity through the perforated plate and the cavity depth of the liner. Therefore the boundary condition or wall impedance is a function of the bias-flow Mach number and the depth of the liner cavity, i.e.,

$$z_a = f(M_{\text{bias}}, L) \tag{30}$$

A detailed description of Eq. (30) is available in Refs. 9 and 10.

Numerical Results

In this study, a numerical simulation has been carried out on a single blade row. The blade moment and lift coefficients are calculated under different wall-impedance conditions and then are plotted as functions of interblade phase angle, inlet Mach number of compressor mean flow, cavity depth of liner, and bias-flow Mach number through the orifice of the liner. In addition, the following results related to the moment coefficient are referred to as axis positions at the leading-edge point.

Figure 2 shows the influence of the interblade phase angle on the blade moment coefficients under various wall impedances. From this plot it is seen that the interblade phase angle has a different influence on the blade moment coefficients under different wall-impedance condition. For the hard-wall condition, the blade remains unstable for most interblade phase angles between 0 and 2π. The blade can remain stable for most interblade phase angles under specific soft-wall conditions such as soft wall 1 ($M_{\text{bias}} = 0.07$, $L = 0.1$) and soft wall 2 ($M_{\text{bias}} = 0.07$, $L = 0.15$). However, still at some interblade phase angles, the soft wall makes the blade become more unstable, for example, $\sigma = 4.5$.

Figure 3 shows the influence of inlet Mach number on the blade moment coefficient under various wall-impedance conditions. It is noted from this figure that with the variation of inlet Mach number the soft wall and the hard wall have different influencs on blade stability. At most inlet Mach number points, the soft wall makes the blade, which is unstable under the hard-wall condition, become stable. Still, at some Mach number points, the soft wall has little influence on the blade stability. A few points become even more unstable under the soft-wall condition.

Figure 4 shows the influence of the change of liner cavity depth on the blade moment coefficient. The variation of liner cavity depth mainly changes the reactance of the liner. Therefore this figure indeed shows the influence of liner reactance variation on the blade moment coefficient. Figure 5 shows the influence of the bias-flow Mach number variation on the blade moment coefficient. The

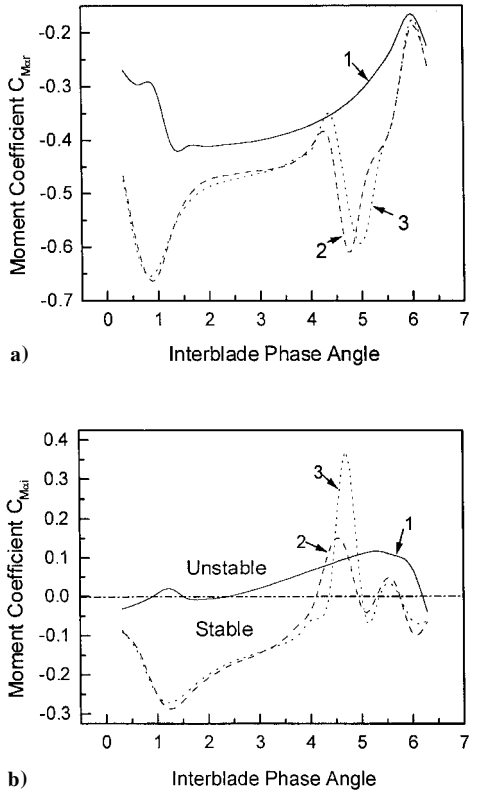

Fig. 2 Moment coefficients are plotted as functions of the interblade phase angle under various wall impedances: a) real part, b) imaginary part of the moment coefficient; $\lambda = 0.1$, $\theta = 35$ deg, space/chord = 3.8, span/chord = 4.0, $M_r = 0.8$. Curve 1, hard wall; curve 2, soft wall ($M_{\text{bias}} = 0.07$, $L = 0.1$); curve 3, soft wall ($M_{\text{bias}} = 0.07$, $L = 0.15$).

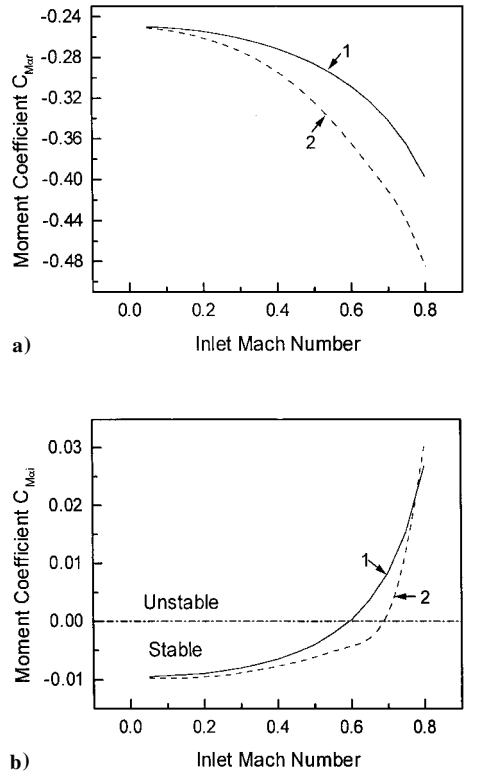

Fig. 3 Moment coefficients are plotted as functions of inlet Mach number under various wall impedances: a) real part, b) imaginary part of the moment coefficient; $\lambda = 0.1$, $\theta = 35$ deg, space/chord = 3.8, span/chord = 4.0, $\sigma = 3.14$, curve 1, hard wall; curve 2, soft wall ($M_{\text{bias}} = 0.05$, $L = 0.1$).

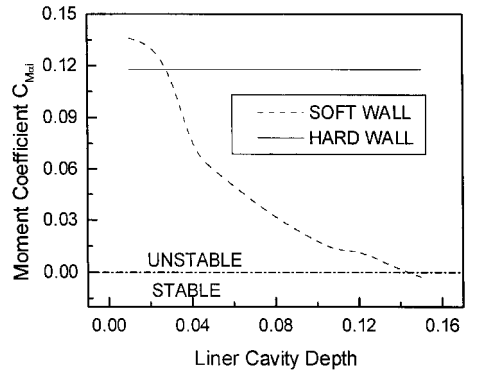

Fig. 4 Effect of liner cavity depth variation on the blade moment coefficient; $\lambda = 0.1$, $\sigma = 5.34$, $\theta = 35$ deg, space/chord = 3.8, span/chord = 4.0, $M_r = 0.8$.

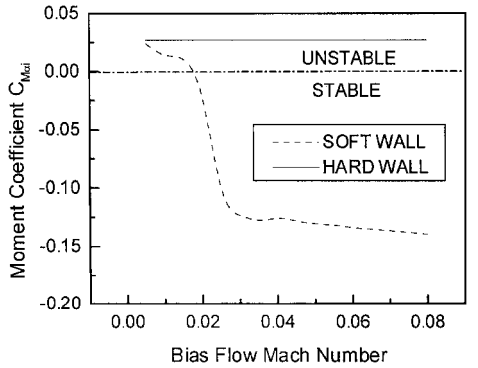

Fig. 5 Effect of bias-flow Mach number variation on the blade moment coefficient; $\lambda = 0.1$, $\sigma = 3.14$, $\theta = 35$ deg, space/chord = 3.8, span/chord = 4.0, $M_r = 0.8$.

variation of the bias-flow Mach number mainly changes the resistance of the liner. So this figure indeed shows the influence of liner resistance variation on the blade moment coefficient. It can be seen from these two figures that, under the hard-wall condition, the blade is unstable, but with a change of liner cavity depth or a variation in the bias-flow Mach number, at one point, such as $L = 0.14$ or $M_{\text{bias}} = 0.02$, the blade begins to become stable. Therefore, in a sense, both resistance and reactance have the same effect on changing the blade stability.

It can be seen from the above figures that the variation of wall impedance has a great influence on the blade moment coefficient. However, it should be also noted that the soft-wall-impedance conditions do not always enhance the blade stability. For the same compressor working condition, some wall-impedance conditions make the blade become stable, whereas other wall-impedance conditions have little effect on blade instability or even make the blade become more unstable. Therefore, how to find an optimal wall-impedance condition and realize it under any given compressor working condition so that the blade can always keep stable is a problem of concern in this paper.

Control Strategy for Smart-Casing Treatment

As has been shown in the preceding section, an optimal acoustic treatment for the compressor casing can suppress blade flutter effectively. However, because of the variations in compressor working conditions, the casing acoustic treatment cannot always remain optimal. Therefore, in order to suppress blade flutter under any compressor working conditions, a smart-casing treatment is necessary, that is, by an active-control method to change the compressor wall acoustic impedance to match with a specific compressor working condition, the blade flutter can always be suppressed. However, how to realize this active control is another problem that should be addressed in this paper. Compared with airfoil flutter, compressor blade flutter often occurs more quickly. Therefore, the existing feedback-control strategies would have a great difficulty to overcome providing they are used to control compressor blade flutter. Obviously some other more effective control strategies should be found for compressor blade flutter control.

A natural choice is to actively adjust the wall impedance. In fact, there are two controllable variables for the liner discussed in this paper. One is the liner cavity depth; the other is the bias-flow Mach number through the orifices of the liner. When these two variables are combined, any required wall-impedance condition can be obtained, as shown in Ref. 10. To keep the blade stable, the wall-impedance condition should be adjusted with the variation of the compressor working condition. For a specific compressor, interblade phase angle and inlet mean-flow Mach number are the two main parameters that determine the blade aeroelastic stability. Once one of them changes, the compressor aerodynamic damping also changes. Therefore this will influence the stability of the compressor blade. No doubt there are other factors that are related to the blade flutter. In this paper, emphasis is placed on the effect of interblade phase angle and mean-flow condition. Naturally the objective of active control is to keep the compressor blade stable under any interblade phase angle and inlet mean-flow Mach number. To realize this objective, the optimal wall impedance matched with the corresponding interblade phase angle and inlet mean-flow Mach number should be found.

It has been discussed above that the imaginary part of the blade moment coefficient reflects the blade stability. If the imaginary part of the moment coefficient is negative, the blade is stable; otherwise, it is unstable. A series of three-dimensional plots that show the imaginary part of blade moment coefficient as a function of liner cavity depth and bias-flow Mach number at some specific mean- flow Mach numbers and interblade phase angles are given by numerical calculations. For each three-dimensional plot, the minimal point of the plot is the optimal point for the wall acoustic impedance to match with the compressor working condition. At this point the blades remain in the most stable status. Therefore, the optimal values of liner cavity depth and bias-flow Mach number for control can be determined by this point. Figures 6 and 7 give the three-dimensional plots at different mean-flow Mach numbers and interblade phase

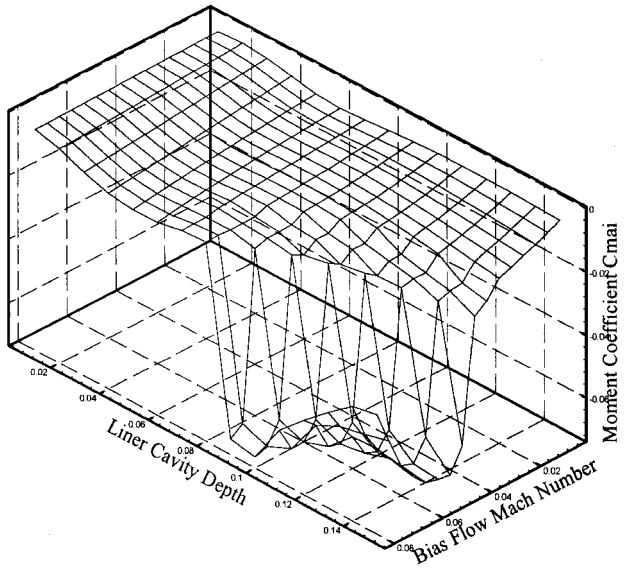

Fig. 6 Moment coefficient $C_{M\alpha i}$ as a function of liner cavity depth and bias-flow Mach number; $\lambda = 0.1$, $\sigma = 3.14$, $\theta = 35$ deg, space/chord = 3.8, span/chord = 4.0, $M_r = 0.5$.

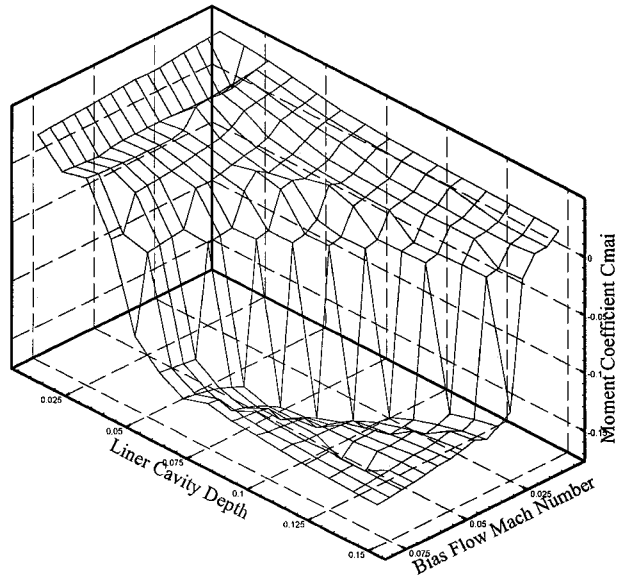

Fig. 7 Moment coefficient $C_{M\alpha i}$ as a function of liner cavity depth and bias-flow Mach number; $\lambda = 0.1$, $\sigma = 3.14$, $\theta = 35$ deg, space/chord = 3.8, span/chord = 4.0, $M_r = 0.8$.

angles, respectively. Correspondingly, the plots at other mean-flow Mach numbers and interblade phase angles can also be obtained. Once the optimal point for each plot is found, then the optimal curves of blade moment coefficient as functions of the inlet mean-flow Mach number and the interblade phase angle can be obtained. Because of the complexity of the phenomenon involved, this paper deals with the variation of the inlet mean-flow Mach number and the interblade phase angle separately. Figure 8 shows the optimal blade moment coefficient as a function of the inlet mean-flow Mach number when the interblade phase angle is fixed. Figure 9 shows the optimal blade moment coefficient as a function of interblade phase angle when the inlet mean-flow Mach number is fixed. At the same time, the optimal curves for wall impedance and control values for liner cavity depth and bias-flow Mach number as functions of the inlet mean-flow Mach number and interblade phase angle can also be obtained, as shown in Figs. 10–13, respectively.

According to the control curves in Figs. 12 and 13, as long as the compressor mean-flow Mach number and the interblade phase angle are known, the control values of the bias-flow Mach number

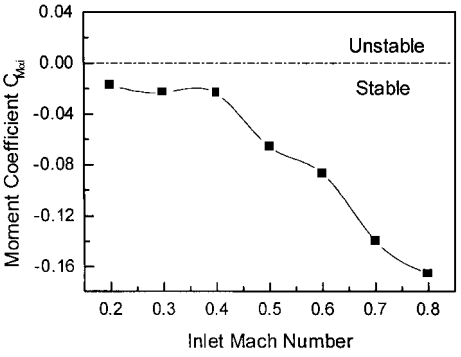

Fig. 8 Optimal blade moment coefficient as a function of inlet mean-flow Mach number; $\lambda = 0.1$, $\sigma = 3.14$, $\theta = 35$ deg, space/chord = 3.8, span/chord = 4.0.

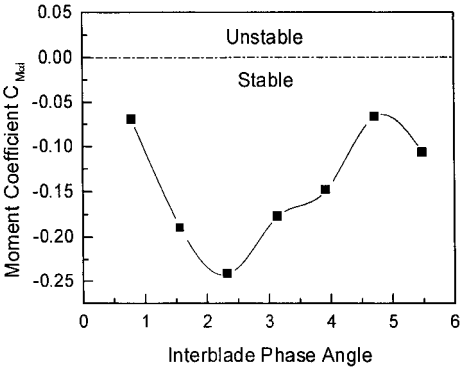

Fig. 9 Optimal blade moment coefficient as a function of interblade phase angle; λ =0.1, $M_r = 0.7$, $\theta = 35$ deg, space/chord = 3.8, span/chord = 4.0.

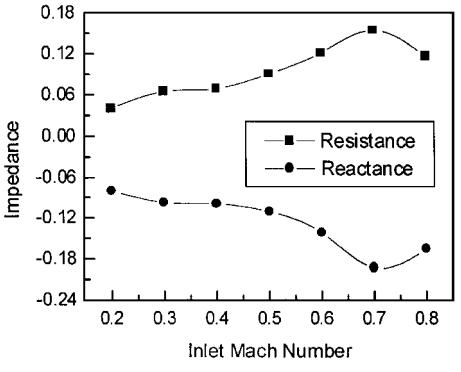

Fig. 10 Optimal wall impedance as a function of inlet mean-flow Mach number.

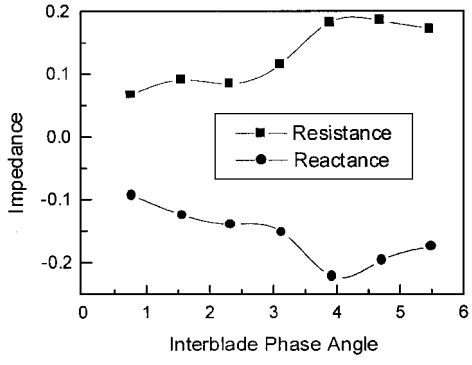

Fig. 11 Optimal wall impedance as a function of interblade phase angle.

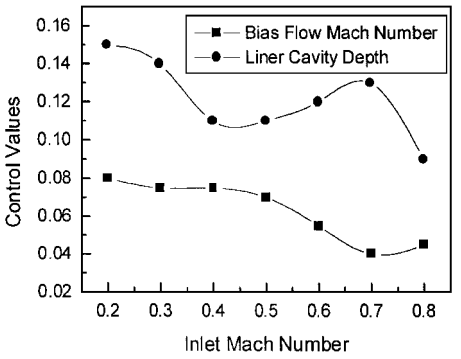

Fig. 12 Control value of bias-flow Mach number and liner cavity depth as functions of inlet Mach number.

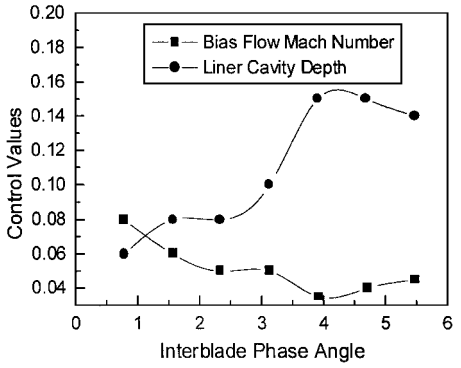

Fig. 13 Control value of bias-flow Mach number and liner cavity depth as functions of interblade phase angle.

Fig. 14 Feedforward-control system for smart-casing treatment.

and the liner cavity depth can be obtained from these curves. If these controllable variables of the liner are adjusted to their corresponding control values, the impedance condition required for making the compressor blade stable can be satisfied. The control can be realized by a feedforward-control system, illustrated in Fig. 14. Compared with traditional feedback-control strategies that have been applied to airfoil flutter control, this control system can respond before any flutter precursor is formed on the compressor blade. Therefore blade flutter can never happen under such conditions.

Conclusions

A soft wall as a kind of casing treatment was suggested to suppress compressor flutter a couple of years ago. However, any given soft wall has to be designed to match with a specific compressor working condition. As long as this working condition changes, for example, the inlet mean-flow Mach number or the interblade phase angles varies, the optimal flow condition under which the soft wall works well to suppress compressor blade flutter cannot be satisfied anymore. That is, the boundary condition is not a good match with such a flow condition to control the flutter effectively. In this paper a smart casing as a new concept of casing treatment is proposed. It is achieved by an active-control method. A kind of acoustic liner with adjustable impedance is introduced as the actuator to change the wall boundary condition. In the present study the optimal impedance condition required for suppressing compressor blade flutter and corresponding control values for liner cavity depth and bias-flow Mach number are given numerically. With active control, the blade flutter can be suppressed under any compressor working condition. It should be pointed out that all the results given in this paper are obtained based on the numerical simulations. For practical

applications, an experimental verification of the proposed control strategies is necessary.

Acknowledgment

The financial support of the National Natural Science Foundation of China (No. 59925616) is gratefully acknowledged.

References

[1]Bendiksen, O. O., "Recent Developments in Flutter Suppression Techniques for Turbomachinery Rotors," *Journal of Propulsion and Power*, Vol. 4, No. 2, 1988, pp. 164–171.

[2]Watanabe, T., and Kaji, S., "Possibility of Cascade Flutter Suppression by Use of Nonrigid Duct Wall," *Proceedings of the Third International Symposium on Aeroelasticity in Turobomachines*, edited by D. S. Whitehead, Cambridge Univ. Press, Cambridge, England, 1984, pp. 261–276.

[3]Namba, M., Yamsaki, N., and Kurihara, Y., "Some Three-Dimensional Effects on Unsteady Aerodynamic Forces on Oscillating Cascades," *Proceedings of the Third International Symposium on Aeroelasticity in Turobomachines*, edited by D. S. Whitehead, Cambridge Univ. Press, Cambridge, England, 1984, pp. 217–230.

[4]Sun, X., and Kaji, S., "Effects of Wall Admittance Changes on Aeroelastic Stability of Turbomachinery," *AIAA Journal*, Vol. 38, No. 9, 2000, pp. 1525–1533.

[5]Huang, X. Y., "Active Control of Airfoil Flutter," *AIAA Journal*, Vol. 25, No. 8, 1987, pp. 1126–1132.

[6]Howe, M. S., "On the Theory of Unsteady High Reynolds Number Flow through a Circular Aperture," *Proceedings of the Royal Society of London A*, Vol. 366, 1979, pp. 205–223.

[7]Bechert, D. W., "Sound Absorption Caused by Vorticity Shedding, Demonstrated with a Jet Flow," *Journal of Sound and Vibration*, Vol. 70, No. 3, 1980, pp. 389–405.

[8]Hughes, I. J., and Dowling, A. P., "The Absorption of Sound by Perforated Linings," *Journal of Fluid Mechanics*, Vol. 218, 1990, pp. 299–335.

[9]Jing, X., and Sun, X., "Experimental Investigations of Perforated Liners with bias Flow," *Journal of the Acoustical Society of America*, Vol. 106, No. 5, 1999, pp. 2436–2441.

[10]Zhao, H., and Sun, X., "Active Control of Wall Acoustic Impedance," *AIAA Journal*, Vol. 37, No. 7, 1999, pp. 825–831.

[11]Goldstein, M., *Aeroacoustics*, McGraw–Hill, New York, 1976, pp. 28–31.

[12]Ko, S. H., "Sound Attenuation in Acoustically Lined Circular Ducts in the Presence of Uniform Flow and Shear Flow," *Journal of Sound and Vibration*, Vol. 22, No. 2, 1973, pp. 193–210.

[13]Smith, S. N., "Discrete Frequency Sound Generation in Axial Flow Turbomachines," Great Britain Aeronautical Research Council R&M 3709, March 1972.